Environ. Health Pollut. Res., 2026, 1(2), 84-96

Environmental Health and Pollution Research

Homepage: www.ehpr.ir



ISSN: 3115-9281

Stabilization and solidification of electroplating sludge in cement-based mortars: effects of rice husk ash on compressive strength and heavy-metal leachability

Sahar Shams [1]✉, Saeid Gitipour [1], and Majid Baghdadi [1]

[1]Department of Environmental Engineering, Faculty of Environment, University of Tehran, Tehran, Iran

ARTICLE INFO

Paper Type: Research Paper

Received: 09 July 2026
Revised: 11 August 2026
Accepted: 13 August 2026
Published: 13 August 2026

Keywords
Compressive Strength
Electroplating Sludge
Heavy-Metal Leaching
Rice Husk Ash
Stabilization/Solidification

Corresponding author:
S. Shams
✉saharshams@ut.ac.ir

ABSTRACT

Electroplating generates large volumes of heavy-metal-bearing sludge whose secondary environmental burden can exceed that of the wastewater itself, yet a unified, reliably safe disposal route is still lacking. This study examined the stabilization/solidification (S/S) of electroplating sludge (ES) in cement-based mortars and assessed rice husk ash (RHA) as a complementary matrix for immobilizing the contained metals. Twelve mortar mixes were prepared: a plain Portland cement mortar (mix F) and eleven mixes organized into three groups, comprising ES introduced into the binder phase at 0-75 % of the cement mass together with RHA at 5 % (Group A) or 10 % (Group B) of the cement mass, and ES used as a partial fine-aggregate replacement at 15-35 % by volume (Group C). Fresh-state behavior (slump, setting time, specific gravity), unconfined compressive strength at 7, 28 and 90 days, and the leaching of Cd, Pb, Ni, Cr, As and Cu were measured. Replacing fine aggregate with ES raised the slump from 75 to 150 mm, whereas increasing the ES content of the binder progressively retarded setting, an effect amplified by a higher RHA content. Compressive strength fell sharply once ES entered the binder, from 16.3-29.0 MPa for the sludge-free mixes to 0.30-6.1 MPa at ES/CEM ratios of 25-75 %, and the 28- and 90-day values were almost identical, so that no late-age recovery should be expected. Used as a fine aggregate, ES was far less damaging, with the mortars retaining 22-53 % of the control strength. Leaching tests conducted under an identical protocol on the raw sludge and on the mortars showed that Cd, Pb and As were immobilized below their US EPA regulatory levels, whereas Cr remained above the 5 mg/L limit in every sludge-bearing mix. The results delimit the loadings over which ES can be incorporated into cementitious materials and identify chromium leaching as the principal constraint on safe reuse.

Highlights

- Electroplating sludge was stabilized in cement mortars with rice husk ash.
- Raw sludge exceeded regulatory limits for every heavy metal measured.
- Compressive strength fell sharply as sludge replaced cement in the binder.
- Using sludge as fine aggregate preserved higher strength and workability.
- Cd, Pb, and As were immobilized, but Cr leaching exceeded the limit.

Citing:
Shams, S., Gitipour, S. & Baghdadi, M. (2026). Stabilization and solidification of electroplating sludge in cement-based mortars: effects of rice husk ash on compressive strength and heavy-metal leachability. *Environmental Health and Pollution Research*, 1(2), 84-96. doi: 10.22034/ehpr.2026.590342.1015

1. Introduction

The rapid expansion of industrial activity over recent decades has markedly increased human exposure to heavy metals, and even low environmental concentrations are now recognized as a serious threat to public health (Balali-Mood et al. 2021). Among the principal anthropogenic sources, the electroplating industry is especially problematic because hazardous metal

ions such as copper (Cu), nickel (Ni), chromium (Cr) and lead (Pb) are routinely discharged in its wastewater and are readily taken up by living organisms (Rajoria et al. 2021). Electroplating and surface-treatment operations generate large volumes of chemically complex wastewater (Wang H et al. 2024), and when this is discharged without adequate treatment it can give rise to toxic metal–organic complexes that pose long-term ecological risks. A range of treatment technologies has accordingly been developed and refined, including chemical precipitation, adsorption, coagulation, flocculation, ion exchange, electrocoagulation, membrane filtration and biorecovery (Kamar et al. 2024).

Despite this diversity, conventional treatment routes are frequently constrained by high capital and operating costs and by the difficulty of handling and disposing of the resulting sludge (Rajoria et al. 2021), so that the complete removal of toxic metals from industrial effluents remains a persistent challenge (Adenuga et al. 2019). Advanced oxidation processes (AOPs), originally developed in the 1980s for drinking-water applications, have more recently attracted attention for the destruction of persistent organic pollutants in wastewater (Deng and Zhao 2015; Momotko et al. 2025). Even so, the variable composition and high contaminant load of electroplating wastewater often lead to incomplete metal removal during treatment (Rajoria et al. 2025), and an estimated 2–20 % of the chemicals and metals used in the process are leached into the wastewater stream (Rajoria et al. 2021). Reducing the environmental footprint of this sector therefore requires complementary strategies that address not only the liquid effluent but also the solid residues generated during its treatment.

A particularly important issue in this respect is the large quantity of metal-bearing sludge produced during the treatment of electroplating wastewater, which is classified as highly toxic and hazardous (Yu et al. 2022). The secondary environmental burden associated with this sludge is, in many respects, greater than that of the wastewater itself, and at present no unified and reliably safe disposal route exists (Wang H et al. 2024). Current management practices for such hazardous residues include thermal treatment, bioremediation, electrochemical treatment, chemical precipitation and stabilization/solidification (S/S) (Wang J et al. 2025). Among these, S/S has become a well-established and versatile technology for rendering contaminated wastes harmless and enabling their reuse (Chen et al. 2020; Petrillo et al. 2025). During the S/S process, cement hydration generates a crystalline matrix that physically entraps the contaminants within the sludge (Chen et al. 2009), and the incorporation of industrial byproducts as secondary raw materials in such systems is consistent with the principles of the circular economy (Monosi et al. 2016).

Portland cement (PC) remains the most widely used binder for S/S applications (Ouhadi et al. 2021), yet its manufacture is energy-intensive and releases large amounts of carbon dioxide (CO_2), dust, sulfides, and nitrogen compounds, contributing to several pressing global environmental problems (Miao et al. 2025). The partial replacement of PC by industrial or agricultural byproducts has therefore gained increasing attention as an environmentally safer, mechanically stable, durable and economically attractive alternative (Chiu et al. 2019). Rice husk ash (RHA) is a particularly relevant candidate in Iran, where husk accounts for approximately 23 % of the mass of the paddy grain and more than 0.5 million tonnes are generated each year, principally in the northern rice-growing provinces; at the ash yields typical of combustion, of the order of 18–20 % by mass, this corresponds to an annual RHA potential on the order of 10^5 tonnes (Yaghoubi et al. 2019). Most of this residue is presently directed to low-value routes such as combustion for rice drying and domestic heating, use as animal feed, mulching material and soil amendment, or is disposed of by open burning, while the ash that remains has historically had no application and has commonly been discharged to water streams (Yaghoubi et al. 2019). A multicriteria assessment carried out for Guilan Province nevertheless ranked industrial valorization as the most appropriate use of the husk and disposal by burning as the least appropriate (Yaghoubi et al. 2019), so that conversion of the ash into a construction material is consistent with national waste-management priorities.

This role is underpinned by the chemistry of the material, which consists predominantly of silica (Della et al. 2002). Where combustion is controlled, that silica is retained in a largely amorphous, porous and high-surface-area form which reacts with the calcium hydroxide released during cement hydration to precipitate additional calcium silicate hydrate (C-S-H) and to refine the pore structure of the hardened matrix. Its reactivity is not an intrinsic property, however, but varies with the final combustion temperature and its duration, the heating and cooling regimes, the type of kiln and the fineness of grinding, as well as with the rice variety, the moisture content of the husk and the geographical origin of the material (Chandrasekhar et al. 2003). RHA has accordingly been examined in numerous studies as a mineral additive capable of enhancing the performance of cement-based systems (Asavapisit and Macphee 2007), and recent Iranian work confirms its pozzolanic contribution to the strength and durability of high-performance and self-compacting concretes produced with locally available materials (Ziyari and Mostakhdemin Hosseini 2025; Fathollahi et al. 2025; Momeni and Ghorbani Kamsari 2025). Its usefulness extends to S/S matrices specifically, having been assessed for the solidification/stabilization of heavy-metal-contaminated slurry (Chiu et al. 2019), while Chen et al. (2022) showed that modified RHA can act as an eco-friendly binder for the effective stabilization of waste clay in road-construction applications, further supporting its potential as a low-carbon alternative to PC. Despite this evidence, and despite domestic interest extending back several decades (Jafarpour et al. 1997), the industrial valorization of rice husk ash in Iran has so far remained limited.

Building on these developments, a growing body of research has examined the stabilization and beneficial reuse of metal- and sewage-derived sludges in construction materials, using a wide range of binder systems and producing outputs as varied as cement clinkers, structural and decorative mortars, fired clay bricks and ceramics, concrete paving and paver blocks, subgrade backfill and dedicated matrices for the encapsulation of heavy metals.

Given the heterogeneous and chemically reactive nature of plating sludge, important questions remain regarding the technical specifications of the resulting cementitious product, in particular its strength development and long-term leaching

behavior, and a systematic evaluation of these aspects represents a novel contribution of this study. Within this framework, the present study investigates the feasibility of incorporating electroplating sludge into cementitious mortars and evaluates rice husk ash as a complementary matrix for immobilizing the heavy metals it contains. Specifically, the work assesses the influence of the sludge, introduced either into the binder phase alongside RHA or as a partial replacement for the fine aggregate, on the fresh-state behavior, the compressive strength, and the leaching behavior of the resulting stabilized products, in line with the broader move towards sustainable construction practices based on the valorization of industrial and agricultural byproducts.

2. Materials and Methods

2.1 Raw materials collection and preparation

Ordinary Portland cement (OPC) was used as the principal binder, rice husk ash (RHA) as a supplementary cementitious material, and electroplating sludge (ES) either as a component of the binder phase or as a partial fine-aggregate replacement. The origin of each constituent and the treatment applied to it before mixing are described below.

2.1.1 Electroplating sludge

The electroplating sludge was collected from the sludge-dewatering unit of the Pirouz Shomal industrial wastewater treatment plant, which treats effluents generated by electroplating operations. The sludge is the metal-bearing precipitate separated during the treatment of chromium and nickel plating baths and of the associated rinse waters. Detailed information on the configuration of the treatment train that produced the sludge was not released by the plant operator and is therefore not reported here. The material was collected as a wet filter cake, homogenized and kept in sealed containers so that its moisture content remained unchanged until characterization.

The as-received cake contained approximately 49 % of free water (Section 2.2.2) and was therefore oven-dried at 64 °C to constant mass before mix proportioning; the reason for selecting this temperature is given in Section 2.2.2. After drying, the cake was disaggregated by hand in a laboratory mortar with a pestle until the agglomerates were completely broken down. No mechanical milling, air classification or sieving was applied, so the sludge was introduced into the mortars with its natural grain-size distribution, which is reported in Section 2.2.3.

2.1.2 Rice husk ash

The rice husk was obtained from a local supplier in the city of Ilam and was calcined in an electric laboratory furnace at 550 to 600 °C for 6 h. This temperature window was selected because it is high enough to burn off the organic fraction of the husk but remains below the range in which the silica crystallizes into cristobalite and tridymite, so that the ash retains the amorphous silica responsible for its pozzolanic activity. After calcination, the ash was cooled to ambient temperature, hand-ground in a mortar to break down the residual husk skeleton, and stored in sealed containers until use. The mineralogy and the fineness of the ash were not determined; this limitation is discussed in Section 3.6.

2.1.3 Cement and fine aggregate

The binder was an ordinary Portland cement produced by the Hegmatan Cement Company (Hamedan, Iran), and the fine aggregate was standard sand conforming to DIN EN 196-1 (2016). Both materials were used as received, without any further treatment.

2.1.4 Superplasticizer

A commercial high-range water-reducing admixture was used to restore a comparable consistency in the sludge-bearing mixes of Groups A and B, in which the water/binder ratio falls sharply as the sludge dosage increases (Section 2.3). It was added at 0.20-0.65 % of the cement mass; the individual dosages are given with the mix proportions in Section 2.3. No admixture was used in mix F or in the mixes of Group C.

2.2 Materials characterization

2.2.1 Chemical composition

The chemical compositions of the three constituents were determined by X-ray fluorescence (XRF) spectrometry; the corresponding oxide contents are reported in Table 2 together with the relevant limits of ASTM International C618-05 (2005).

Table 1 Chemical composition (wt %) of OPC, RHA and ES, with the relevant limits of ASTM International C618-05 (2005) for natural pozzolans

Chemical compound	OPC	RHA	ES	ASTM C618 limit
SiO_2	21.90	92.90	9.35	-
Al_2O_3	6.27	3.25	16.12	-
Fe_2O_3	3.48	0.77	1.63	-
$SiO_2 + Al_2O_3 + Fe_2O_3$	31.65	96.92	27.10	min. 70
CaO	59.26	0.94	9.92	-
MgO	1.03	1.01	1.14	-
Na_2O	0.02	0.29	0.86	-
K_2O	0.80	2.54	0.15	-
SO_3	2.35	2.50	2.35	max. 4
LOI	4.14	3.60	33.94	max. 10

As shown in Table 1, RHA satisfies the ASTM International C618 requirements for natural pozzolans, with a combined $SiO_2 + Al_2O_3 + Fe_2O_3$ content of 96.92 % (≥ 70 %), an SO_3 content of 2.50 % (≤ 4 %), and a loss on ignition of 3.60 % (≤ 10 %). In contrast, ES does not meet the pozzolanic threshold, with a summed oxide content of only 27.10 % and an unusually high loss on ignition of 33.94 %. ES therefore cannot be regarded as a conventional pozzolan and was investigated primarily as a candidate matrix for the stabilization/solidification of its heavy-metal content rather than as an active mineral additive. It should be noted that the oxides listed in Table 1 account for the great majority of the OPC but for only about three-quarters of the ES; the balance is made up of the heavy-metal oxides, principally those of chromium, nickel, copper and zinc, which are the reason for classifying the material as hazardous and whose concentrations are reported in Section 3.1 rather than as oxide equivalents.

2.2.2 Moisture content of the sludge

Because the as-received electroplating sludge contained a substantial fraction of free water, its moisture content was determined gravimetrically prior to mix proportioning. Three replicate subsamples of the homogenized sludge were placed in tared crucibles, dried to constant mass at 64 °C and reweighed. A drying temperature of 64 °C was chosen in preference to the more common 105 °C so that free water would be fully removed while minimizing the loss of volatile and thermally labile metal species, in particular Hg compounds and the oxyhydroxide-bound water associated with the precipitated heavy-metal phases, thereby preserving the composition reported in Table 1. The average data are summarized in Table 2.

Table 2 Gravimetric determination of the moisture content of the as-received electroplating sludge (mean of three replicate determinations)

Parameter	Value
Container mass (g)	12.897
Container + wet sample, before drying (g)	17.118
Container + dry sample, after drying (g)	15.048
Wet sample mass (g)	4.221
Dry sample mass (g)	2.151
Mass of water lost (g)	2.070
Moisture content, wet basis (%)	≈ 49

The moisture content, calculated on a wet-mass basis (2.070 / 4.221 × 100), was approximately 49 %, confirming that the as-received material was a wet paste rather than a granular solid. To remove any associated uncertainty in the mixing-water content and in cement hydration, the sludge was fully oven-dried at 64 °C before incorporation in the mixes.

2.2.3 Particle-size distribution of the sludge

Because the dried sludge is cohesive and tends to form agglomerates, its grain-size distribution was determined by wet sieving, the procedure normally adopted for fine-grained soils, rather than by dry sieving. A representative subsample was first dried at 64 °C for 24 h and broken down with a rubber hammer to the smallest achievable size, so that the distribution reported here corresponds to the disaggregated material rather than to the as-received cake. The material was then placed on a sieve stack comprising the No. 4, 8, 16, 30, 40, 50, 100 and 200 sieves (4.75, 2.36, 1.18, 0.60, 0.425, 0.30, 0.15 and 0.075 mm) and washed with a jet of water, the washing being continued until the water leaving the sieves ran completely clear. The fractions retained on each sieve were subsequently oven dried at 110 °C for 24 h and weighed; the higher temperature is acceptable at this stage because only the mass of each fraction is required, whereas the 64 °C used elsewhere was chosen to preserve the chemical composition. The cumulative passing percentages were calculated and plotted as the grain-size distribution curve shown in Fig. 1, together with the nominal grading of the CEN standard sand specified in DIN EN 196-1 (2016). Wet sieving was preferred because the washing separates particles that would otherwise remain bound to each other, so that every particle passes the sieve at its true size and the resulting curve represents the actual fineness of the material more reliably than one obtained by dry sieving. The analysis resolves the distribution down to the No. 200 sieve (0.075 mm) only; the fraction finer than that size was not subdivided, and the curve of Fig. 1 is therefore truncated at 0.075 mm.

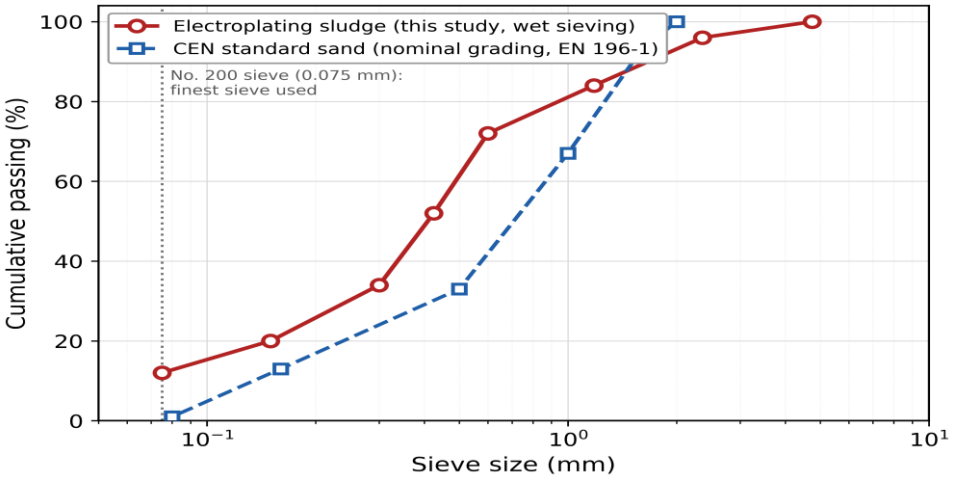


Fig. 1 Grain-size distribution of the electroplating sludge determined by wet sieving, compared with the nominal grading of the CEN standard sand specified in DIN EN 196-1 (2016). The sludge curve is truncated at the No. 200 sieve (0.075 mm), the finest sieve used

The curve confirms that the sludge is a predominantly fine-grained material. The whole of the sample passes the 4.75 mm sieve (No. 4), 96 % passes the 2.36 mm sieve (No. 8), 52 % passes the 0.425 mm sieve (No. 40), 34 % passes the 0.30 mm

sieve (No. 50) and 12 % passes the 0.075 mm sieve (No. 200), so that more than half of the mass is finer than about 0.4 mm. Comparison with the standard sand in Fig. 1 shows that the sludge is the finer of the two materials over the whole range covered: at 0.425 mm the sand passes about 28 % against 52 % for the sludge, and at the finest sieve the sand passes about 1 % against 12 %. The sludge is therefore fine enough to act as a filler in the mixes of Groups A and B and, in Group C, replaces the standard sand with a distinctly finer material.

2.3 Mix proportions and justification

Twelve mortar mixes were prepared: a plain Portland cement mortar, designated F, and eleven mixes organized into three groups, A, B and C. Mix F contains neither ES nor RHA. Because its binder content is identical to that of Group C but differs from that of Groups A and B, mix F serves as the direct reference for Group C and as a general benchmark elsewhere; within Groups A and B, the internal references are mixes A1 and B1, which contain 5 % and 10 % of RHA, respectively, but no sludge, and therefore isolate the contribution of the pozzolanic addition from that of the sludge.

In Groups A and B, the sludge was introduced into the binder phase together with RHA. The RHA content was fixed at 5 wt % of the cement in Group A and 10 wt % in Group B, and the sludge was dosed at 0, 25, 50, and 75 % of the cement mass (ES/CEM). It should be emphasized that the cement content was held constant within each group, at 490 g in Group A and 465 g in Group B, so that the sludge was an addition to the binder phase and not a substitution for the cement; the term "replacement" is therefore avoided for these mixes throughout the paper. One consequence of this design is that, although the water/cement ratio was held at a nominal 0.485, the water/binder ratio computed on the total powder content, cement plus RHA plus sludge, fell from 0.463 to 0.270 in Group A and from 0.440 to 0.261 in Group B as the sludge dosage increased. Both ratios are reported in Table 4, and it is this fall in the water/binder ratio, as much as the water demand of the sludge itself, that made a superplasticizer necessary at ES/CEM ≥ 25 %.

Table 4 Mix proportions of the twelve mortar designs prepared in this study

Group	Mix	ES level (%)[a]	RHA/CEM (%)	Cement (g)	RHA (g)	ES (g)	Sand (g)[c]	Water (g)	w/c[b]	w/b[b]	Super-plasticizer (g)
Control	F	0	0	413	0	0	1350	200	0.484	0.484	0
A	A1	0	5	490	24.5	0	1350	238	0.486	0.463	0
A	A2	25	5	490	24.5	123	1350	238	0.486	0.373	1
A	A3	50	5	490	24.5	245	1350	238	0.486	0.313	3
A	A4	75	5	490	24.5	368	1350	238	0.486	0.270	3
B	B1	0	10	465	46.5	0	1350	225	0.484	0.440	0
B	B2	25	10	465	46.5	116	1350	225	0.484	0.359	1
B	B3	50	10	465	46.5	233	1350	225	0.484	0.302	3
B	B4	75	10	465	46.5	349	1350	225	0.484	0.261	3
C	C1	15	0	413	0	143	1207	200	0.484	0.484	0
C	C2	25	0	413	0	238	1112	200	0.484	0.484	0
C	C3	35	0	413	0	334	1016	200	0.484	0.484	0

[a] For Groups A and B the sludge level is the mass of ES expressed as a percentage of the cement mass (ES/CEM); the cement content is constant within each group, so the sludge is an addition to the binder phase and not a substitution for the cement. For Group C it is the nominal replacement of the fine aggregate on a volume basis, equivalent to 10.6, 17.6 and 24.7 % of the sand by mass; the sand mass was reduced by the mass of sludge introduced. [b] w/c is the ratio of the mixing water to the cement. w/b is the ratio of the mixing water to the total powder content: cement + RHA + ES for Groups A and B, where the sludge is part of the binder phase, and cement + RHA for mix F and Group C, where the sludge acts as an aggregate; [c] The standard sand was batched to ± 5 g.

In Group C, the sludge was used exclusively as a partial replacement for the fine aggregate, at nominal levels of 15, 25 and 35 % defined on a volume basis. Because the sludge is appreciably less dense than the standard sand, these levels correspond to sludge masses of 143, 238 and 334 g, that is 10.6, 17.6 and 24.7 % of the sand by mass. The mass of standard sand was reduced by the mass of sludge introduced, so that the total mass of the granular skeleton was held at 1350 g in every mix, while the cement content, the mixing water and therefore the paste volume were left unchanged and no superplasticizer was added. A nominal water/cement ratio of 0.485 was adopted throughout, and the mortars were prepared in accordance with ASTM International C305-11 (2011). The complete mix proportions are given in Table 4.

The dosage levels were selected to cover as wide an interval as possible rather than to reproduce a single expected optimum. For the sludge introduced into the binder, the ES/CEM ratio was increased in equal steps of 25 % up to 75 %, so that the series spans the whole range from a conservative dosage to a deliberately excessive one. This is consistent with the objective of a stabilization/solidification study, in which the practical question is the maximum waste loading that the binder can accept while still meeting the mechanical and leaching requirements; a narrower range would not have allowed the threshold beyond which performance becomes unacceptable to be identified. For the sludge used as a fine aggregate, the levels of 15, 25 and 35 % were adopted because the material is finer than the standard sand and larger substitutions would appreciably modify the grading of the granular skeleton; the intermediate level of 25 % coincides with the ES/CEM ratio of mixes A2 and B2 and thus permits a direct comparison of the two incorporation strategies at nominally the same sludge content.

The RHA contents of 5 and 10 % lie within the interval usually reported as effective for rice husk ash in cementitious systems and were deliberately kept moderate. Higher contents markedly increase the water demand of the mixture, which at the fixed water/cement ratio of 0.485 would have required superplasticizer dosages large enough to mask the effect of the sludge. Two levels differing by a factor of two are sufficient to show whether the pozzolanic contribution of the RHA compensates for the dilution and the retardation caused by the sludge.

2.4 Testing program

2.4.1 Fresh-state properties

The workability of the fresh mortar was evaluated by the slump test in accordance with ASTM International C143-03 (2003), and the fresh density in accordance with ASTM International C138-09 (2009), the latter being reported below as a specific gravity in g cm^{-3}. The slump cone was preferred to the mortar flow table because the mixes of Group C were highly fluid and because the resulting values are directly comparable with the concrete-based stabilization/solidification literature. The initial and final setting times of the binder phase were measured with the Vicat apparatus in accordance with ASTM International C191-08 (2008), for both the increasing ES and the increasing RHA series, and were compared with the corresponding sludge-free mix of the same group.

2.4.2 Hardened-state properties

The unconfined compressive strength of the mortars was determined on 50 mm cubic specimens in accordance with ASTM International C109/C109M-16a (2016). Tests were carried out at curing ages of 7, 28, and 90 days, with three to four specimens per mix and curing age; the arithmetic mean of the replicates is reported.

2.4.3 Leaching characterization (TCLP)

The leaching behavior was evaluated using the Toxicity Characteristic Leaching Procedure (TCLP) described in US EPA Method 1311 (US Environmental Protection Agency 1992), which simulates the leaching expected if a solidified waste were disposed of in a sanitary landfill and is widely used to determine whether a material can be classified as hazardous. Specimens cured for 28 days were crushed, screened, and contacted with the prescribed acetic acid extraction fluid under continuous end-over-end agitation for the standard duration. The leachates were filtered through a 0.45 µm membrane and split into two aliquots: one for pH determination and one, after acidification, for the analysis of Cu, Ni, Cr, Pb, Cd and As by inductively coupled plasma mass spectrometry (ICP-MS). The same procedure was applied to the raw, oven-dried sludge, so that the leachability of the untreated waste (Section 3.1) and that of the stabilized mortars (Section 3.5) are directly comparable and are expressed on the same basis.

3. Results and Discussion

3.1 Heavy-metal leachability of the raw electroplating sludge

To place the stabilization/solidification program in context, the raw electroplating sludge was itself subjected to the TCLP, and the resulting leachate concentrations were compared with the regulatory levels of the US EPA, the guideline for on-site reuse, the criterion for on-site disposal and the European Union limit values, where available (Table 5). Because the same extraction protocol was applied to the untreated waste and to the stabilized mortars, Table 5 constitutes the baseline against which the leaching results of Section 3.5 are to be read.

Table 5 TCLP leachate concentrations (mg/L) of the raw electroplating sludge, compared with the applicable regulatory thresholds

Heavy metal	TCLP leachate of the raw sludge	US EPA regulatory level[a]	On-site reuse	On-site disposal	EU limit
Pb	45	5	0.75	50	-
Zn	280	[b]	4.3	250	-
Cd	2.8	1	0.11	10	-
Cr	> 1 wt %[c]	5	0.6	50	-
As	11	5	5	50	-
Ni	> 3 wt %[c]	[b]	11	250	0.12
Cu	4125	[b]	-	250	0.6

[a] *US EPA regulatory levels for the toxicity characteristic from US Environmental Protection Agency (1992).*

[b] *Zinc, nickel and copper are not among the eight metals for which a toxicity-characteristic regulatory level is defined (As, Ba, Cd, Cr, Pb, Hg, Se and Ag).* [c] *The leachate concentrations of chromium and nickel were not quantified; the values given are the total contents of the dried sludge (> 10 000 and > 30 000 mg/kg respectively) and are not directly comparable with the leachate-based thresholds in the remaining columns.*

3.2 Fresh-state behavior

3.2.1 Slump

The slump test was carried out on the Group C mixes, in which ES partially replaces the fine aggregate, together with the plain reference mortar F, and the results are plotted in Fig. 2. The slump increased monotonically with the sludge content, from 75 mm for the control to 100, 135 and 150 mm at 15, 25 and 35 % replacement, and the four points are well described by the linear relationship $y = 2.24x + 72.94$ ($R^2 = 0.98$), where y is the slump in mmm and x the volumetric replacement level in percent. Each percentage point of replacement thus raised the slump by about 2.2 mm, even though the water/cement ratio was held at 0.485 and no superplasticizer was used. All the sludge-bearing mixes fall within the range conventionally

regarded as high-workability mortar, indicating that, over this composition range, the partial substitution of fine aggregate by ES does not reduce the workability of the fresh mortar but rather improves it.

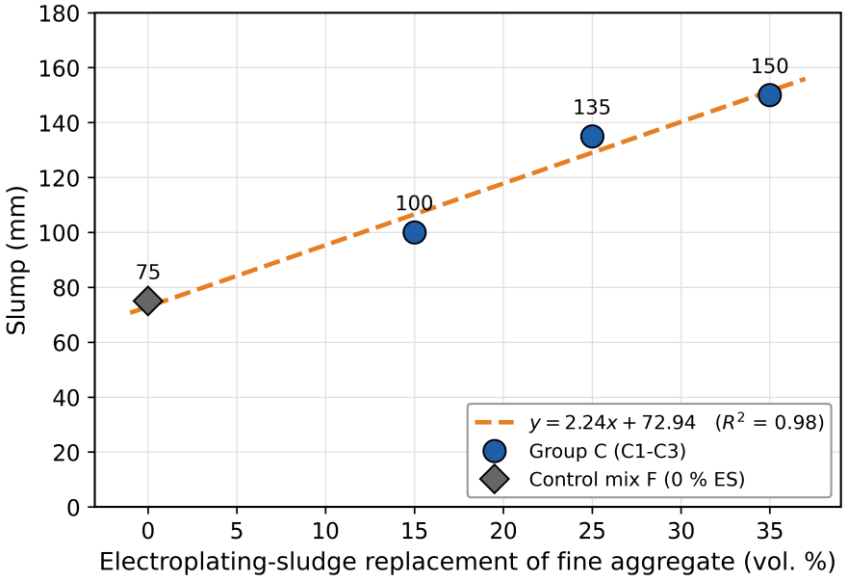


Fig. 2 Slump of the Group C mortars, in which electroplating sludge partially replaces the fine aggregate, together with the plain reference mortar F at 0 % replacement. The fitted line is the least-squares regression through all four points.

The two roles of the sludge act through different mechanisms. When ES is introduced into the binder (Groups A and B), it dilutes the clinker without contributing reaction products of its own, since its combined $SiO_2 + Al_2O_3 + Fe_2O_3$ content is only 27.10 % (Table 2) and it therefore does not meet the compositional requirement for a pozzolan. At the same time its loss on ignition of 33.94 % reflects a large fraction of metal hydroxides, bound water and carbonates, so the particles are internally porous and of high specific surface and retain part of the mixing water instead of releasing it to lubricate the mixture; the metals that pass into the pore solution also precipitate on the cement grain surfaces, a process documented both for cement-solidified electroplating sludge and for cement-treated lead-contaminated clay (Chen et al. 2009; Ouhadi et al. 2021), and modify the early cohesion of the paste. Together with the fall in the water/binder ratio from 0.463 to 0.270 in Group A and from 0.440 to 0.261 in Group B (Section 2.3, Table 4), this is why 1 to 3 g of superplasticizer were required at ES/CEM ≥ 25 % to maintain a comparable consistency.

When ES replaces part of the fine aggregate (Group C), the cement content, the mixing water and therefore the paste volume are unchanged, and only the grading of the granular skeleton is modified. The particle-size distribution measured by wet sieving (Fig. 1) shows that the sludge is markedly finer than the standard sand it replaces, with more than half of its mass finer than about 0.4 mm and 12 % finer than 0.075 mm against about 1 % for the sand. These fines fill the voids between the sand grains and release the water that would otherwise be trapped there, while reducing interparticle friction; the lower specific gravity of the Group C mixes (Table 6) further indicates that, for an equal replaced mass, the porous sludge occupies a larger volume than the sand and increases the volume of fine, paste-like material in the mortar. Both effects raise the flowability and account for the trend in Fig. 2. The two contributions are nevertheless in competition, because the high specific surface of the fines also adsorbs water, so the linear relationship should not be extrapolated beyond 35 % replacement.

Table 6 Specific gravity of the Group C mixes and of the control mortar

Mix code	ES replacement of fine aggregate (vol. %)	Specific gravity (g/cm³)	Change vs control (g/cm³)	Change vs control (%)
F (control)	0	2.145	reference	reference
C1	15	2.085	−0.060	−2.8
C2	25	2.056	−0.089	−4.2
C3	35	2.026	−0.119	−5.6

3.2.2 Setting time

The influence of the ES and RHA contents on the setting behavior of the binder is shown in Fig. 3. Two consistent trends emerge. First, at any fixed RHA content, increasing the proportion of sludge in the binder markedly lengthened both the initial and the final setting times. In Group A the initial set rose from 140 min at 0 % ES to 230, 340 and 400 min at ES/CEM ratios of 25, 50 and 75 %, and the final set from 295 to 390, 470 and 495 min; in Group B the corresponding values were 180, 250, 350 and 420 min for the initial set and 305, 400, 480 and 510 min for the final set. This is consistent with the inhibition of cement hydration commonly reported in the presence of heavy metals, in particular Cu, Cd and Pb, all abundant in the sludge characterized in Table 5, which retard the early hydration of C_3S and C_3A by forming metal hydroxide or metal silicate layers on the cement grain surfaces that delay precipitation of the C-S-H gel (Chen et al. 2009; Chen et al. 2020; Ouhadi et al. 2021). Second, at any given

sludge dosage the mortars containing 10 % RHA set later than their 5 % RHA counterparts, with the initial setting time delayed by 10-40 min and the final setting time by 10-15 min. This RHA-induced retardation is consistent with the slow pozzolanic kinetics of RHA-blended binders: partial substitution of OPC by RHA dilutes the rapidly reacting clinker phases, while the pozzolanic reaction of the amorphous silica with the calcium hydroxide released during hydration is intrinsically slower. The effect is moderate in absolute terms (≤ 40 min on the initial set, ≤ 15 min on the final set), so that practical workability windows are retained at both 5 % and 10 % RHA, even at the highest sludge dosage.

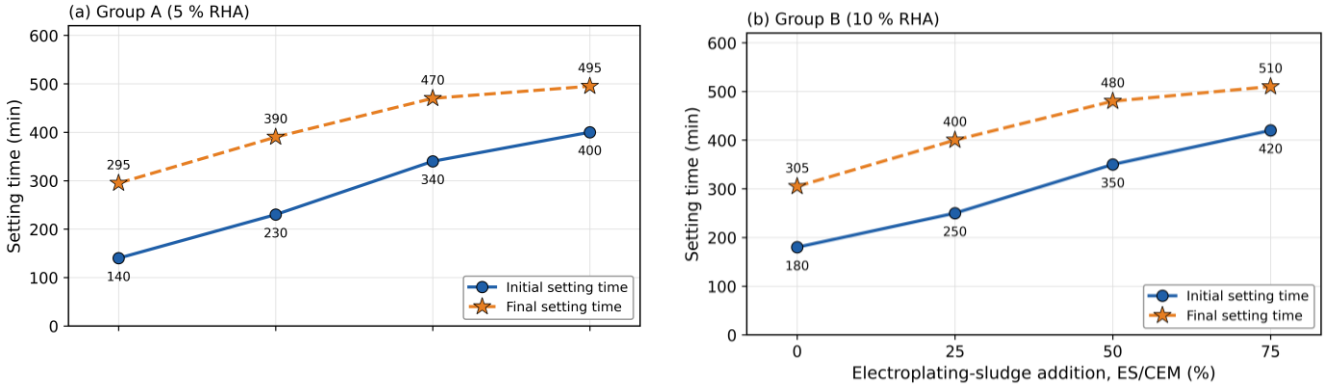


Fig. 3 Initial and final setting times of the binder as a function of the electroplating-sludge dosage: (a) Group A (5 % RHA) and (b) Group B (10 % RHA). The 0 % points correspond to the sludge-free reference mixes A1 and B1.

3.3 Specific gravity

The specific gravity of the Group C mixes decreased steadily as the sludge content increased, from 2.085 g cm^{-3} at 15 % replacement to 2.056 and 2.026 g cm^{-3} at 25 and 35 % respectively (Table 6). Relative to the control mix F (2.145 g/cm³), these are reductions of 0.060, 0.089 and 0.119 g/cm³, about 2.8, 4.2 and 5.6 %. Because Group C and mix F share the same cement content, the same mixing water and the same total mass of granular skeleton, the comparison isolates the effect of the sludge itself. The decrease is consistent with the replacement of dense natural sand by lighter, more porous sludge particles, whose high loss on ignition (33.94 %, Table 2) reflects the hydroxide-rich, low-density character typical of the precipitates produced by electroplating wastewater treatment (Chen et al. 2009; Ouhadi et al. 2021). The change is modest, at most about 6 %, so the partial substitution of fine aggregate by ES lowers the specific gravity of the mixture only slightly.

3.4 Compressive strength

The unconfined compressive strength of the mixes in which sludge was introduced into the binder is shown in Fig. 4a for Group A (5 % RHA) and in Fig. 4b for Group B (10 % RHA), while Fig. 4c compares the fine-aggregate replacement mixes of Group C with the plain reference mortar F at 28 days.

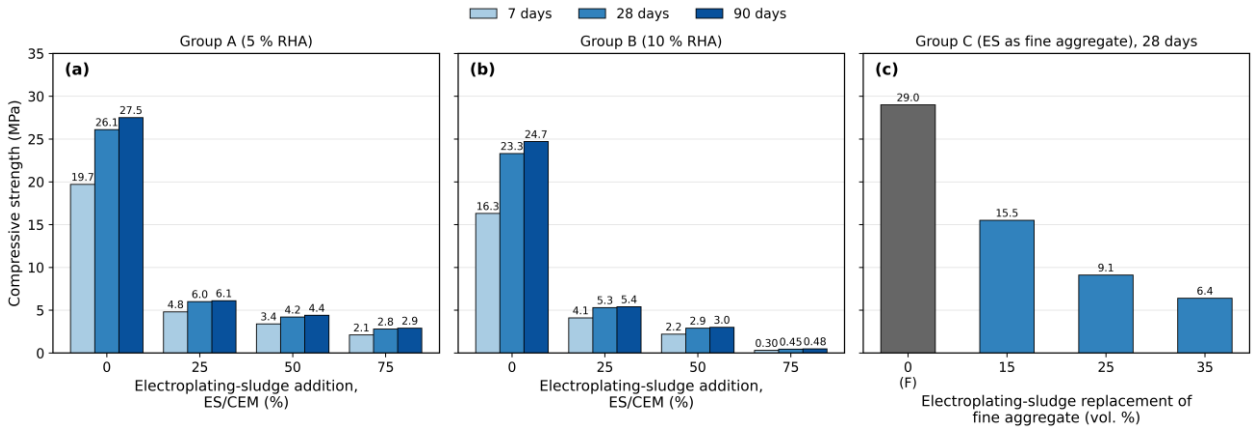


Fig. 4 Unconfined compressive strength of the mortars: (a) Group A (5 % RHA) and (b) Group B (10 % RHA), in which the sludge is added to the binder, at 7, 28 and 90 days; and (c) Group C, in which the sludge replaces part of the fine aggregate, together with the plain reference mortar F, at 28 days.

Before the effect of the sludge is considered, the two sludge-free blended mixes may be compared with the plain control. At 28 days, mix F reached 29.0 MPa against 26.1 MPa for A1 (5 % RHA) and 23.3 MPa for B1 (10 % RHA), so that the pozzolanic addition cost about 10 and 20 % of the 28-day strength even though the cement contents of A1 and B1 exceed that of F. Two factors contribute. The higher total powder content of the blended mixes raises the water demand at a fixed water/cement ratio, and the pozzolanic reaction of the RHA is slow, so that by 28 days it has not yet compensated for the dilution of the clinker; the trend with age supports this interpretation, the 90-day strengths of A1 and B1 recovering to 27.5 and 24.7 MPa. Mix F is therefore used below as the direct reference for Group C, whose binder is identical to it,

while A1 and B1 serve as the internal references within Groups A and B.

For both RHA levels the strength fell steeply once sludge entered the binder. The sludge-free mixes reached 19.7, 26.1 and 27.5 MPa at 7, 28 and 90 days for 5 % RHA (Group A) and 16.3, 23.3 and 24.7 MPa for 10 % RHA (Group B), whereas at ES/CEM = 25 % the 90-day strength dropped to 6.1 MPa (Group A) and 5.4 MPa (Group B), and at 75 % it fell to 2.9 MPa in Group A and 0.48 MPa in Group B. Strength increased with curing age at every dosage, reflecting the slow but continuing development of the binding phases, but the gains were insufficient to offset the dominant effect of the sludge. The steeper loss in Group B indicates that the higher RHA content, while beneficial for pozzolanic refinement in the longer term, further diluted the early strength-giving clinker phases and, combined with the hydration-retarding metals in the sludge, left very little load-bearing capacity at the highest dosage.

The marked strength reduction is attributable to the same mechanisms that retarded setting: the heavy metals interfere with cement hydration (Chen et al. 2009; Chen et al. 2020; Ouhadi et al. 2021), and the high loss on ignition and porous nature of the sludge increase porosity and weaken the matrix; the fall in the water/binder ratio documented in Table 4 also leaves an increasing fraction of the powder unwetted and therefore inert. Reported S/S practice indicates that cement- and lime-based binders dominate the field, with Portland cement generally outperforming lime in compressive and tensile strength, and that an optimal cement dosage of about 6 % has been proposed on economic and engineering grounds (Wang DX et al. 2012); the waste-to-cement ratio in the present mixes was varied between 25 and 75 % to span the range of practical interest.

A further feature of Fig. 4a, b is that the strength gain between 28 and 90 days, which is clear in the sludge-free mixes, almost disappears once sludge is present: at every dosage the two ages give practically the same value, 6.0 against 6.1 MPa at 25 % ES, 4.2 against 4.4 MPa at 50 % and 2.8 against 2.9 MPa at 75 % in Group A, with the same pattern in Group B, so that the 28-day strength is effectively the ultimate strength of these mixes. Three factors combine to produce this plateau. At high ES/CEM ratios, the clinker fraction of the total powder is small and is largely consumed within the first 28 days, leaving little unreacted cement to form further C-S-H. The metal hydroxide and metal silicate layers described in Section 3.2.2 are stable in the pore solution and progressively isolate the residual anhydrous cores, so that hydration is arrested rather than merely delayed and the strength lost to retardation is never recovered at later ages (Chen et al. 2009; Chen et al. 2020). Finally, the precipitation of the metals consumes calcium hydroxide and lowers the alkalinity of the pore solution, which suppresses the pozzolanic reaction of the RHA precisely in the mixes that would benefit most from it, in agreement with the plateau being more pronounced in Group B. Strength in these mixes is therefore governed by a coarse pore structure that later hydration can no longer refine, and no late-age recovery should be expected from sludge-bearing binders.

When ES instead replaced the fine aggregate (Group C, 28-day curing, Fig. 4c), the compressive strengths were 15.5, 9.1 and 6.4 MPa at 15, 25 and 35 % replacement, against 29.0 MPa for the plain reference mortar F, that is retentions of about 53, 31 and 22 % of the control strength. These values are well above those of the mixes in which the sludge entered the binder at a comparable loading; at 25 %, for example, Group C retains 9.1 MPa whereas A2 and B2 retain 6.0 and 5.3 MPa. The binder phase remains intact when ES is used as an aggregate, so hydration is not directly inhibited and the loss of strength arises mainly from replacing a dense, strong sand by weaker and more porous particles, in line with the reduction in specific gravity reported in Table 6. The loss is not proportional over the whole range: the first 15 % of replacement costs about 0.90 MPa per percentage point of sludge, against roughly 0.46 MPa per percentage point between 15 and 35 %, which suggests that once the granular skeleton is dominated by the sludge fines, further replacement has a smaller marginal effect.

3.5 Leaching behavior (TCLP)

The leaching of the stabilized mortars, measured by TCLP on 28-day specimens, is reported in Table 7 and plotted in Fig. 5, which shows the leachate concentrations of Cr, Ni, Cu and Pb against the ES/CEM ratio for (a) Group A (5 % RHA) and (b) Group B (10 % RHA) on a logarithmic scale, together with the US EPA regulatory level of 5 mg/L applicable to chromium and lead. Cadmium and arsenic are not plotted because they lay below the detection limit in all but one determination: arsenic remained below 0.005 mg/L in every mix and cadmium in five of the six, the single exception being mix B4 at 0.1 mg/L, while lead did not exceed 3.0 mg/L in any mix.

Table 7 TCLP leachate concentrations of the stabilized mortars (28-day specimens; mg/L). Group A contains 5 % RHA and Group B 10 % RHA

Mix	ES/CEM (%)	Cd	Pb	Ni	Cr	As	Cu	pH
A2	25	< 0.005	0.1	26.0	9.0	< 0.005	1.8	6.1
A3	50	< 0.005	0.3	44.6	9.7	< 0.005	2.0	5.9
A4	75	< 0.005	1.0	86.6	13.1	< 0.005	2.8	5.7
B2	25	< 0.005	0.4	19.4	5.6	< 0.005	1.0	6.2
B3	50	< 0.005	0.3	41.7	8.5	< 0.005	1.6	5.9
B4	75	0.1	3.0	61.0	11.0	< 0.005	2.0	5.8
US EPA regulatory level	-	1	5	-	5	5	-	-

All three elements are therefore below their respective US EPA regulatory levels (Cd 1, Pb 5, As 5 mg/L; Table 5), indicating effective immobilization by the cementitious matrix. Chromium, by contrast, exceeded the 5 mg/L limit in every sludge-bearing mix, ranging from 5.6 to 13.1 mg/L and increasing with the sludge dosage, so that chromium leaching remains the principal constraint on safe reuse of the products despite the very large reduction relative to the raw sludge (Table 5). Nickel and copper, for which the US EPA does not specify a regulatory level, were released at 19.4-86.6 and 1.0-2.8 mg/L respectively, again rising with the sludge dosage. The eluate pH remained mildly acidic (5.7-6.2), reflecting the buffering imposed by the acetic acid extraction fluid. As Fig. 5 shows, chromium, nickel and copper increase approximately log-linearly with the sludge dosage in both groups; lead follows the same trend in Group A but is non-monotonic in Group B, where the 25 and 50 % mixes are indistinguishable (0.4 and 0.3 mg/L) before a sharp rise to 3.0 mg/L at 75 %.

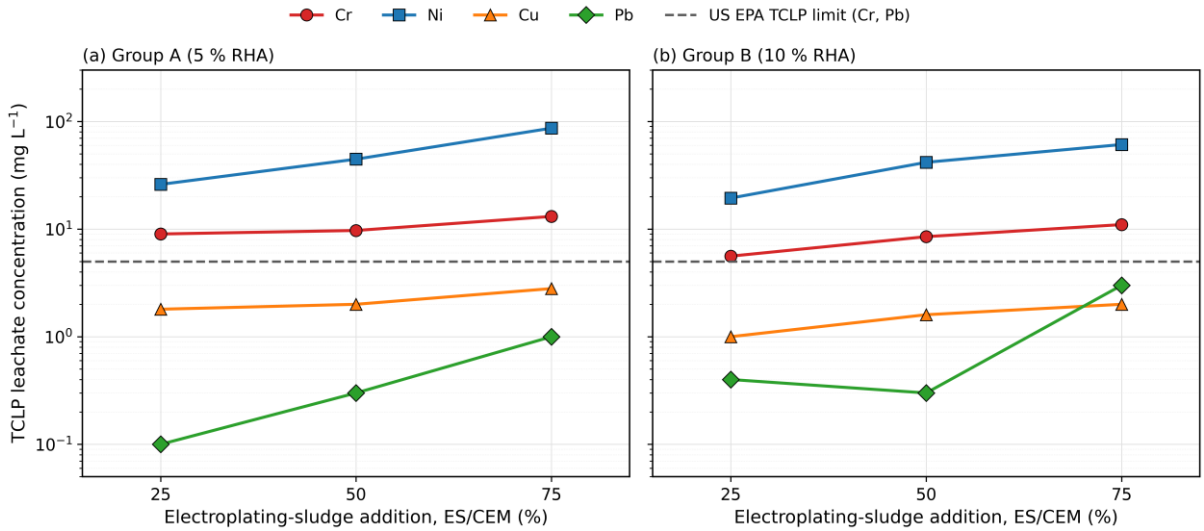


Fig. 5 TCLP leachate concentrations of Cr, Ni, Cu and Pb for the 28-day stabilized mortars as a function of the electroplating-sludge dosage: (a) Group A (5 % RHA) and (b) Group B (10 % RHA). The dashed line is the US EPA regulatory level of 5 mg/L, which applies to chromium and lead but not to nickel or copper. Cadmium and arsenic are omitted because they lay below the detection limit in all but one determination.

The contrast between the elements follows from the way a cement matrix retains them. Cadmium and lead are divalent cations and are held by three mechanisms that all benefit from the alkalinity of the binder: precipitation as sparingly soluble hydroxides and, in the case of lead, as hydroxy carbonate phases; sorption on the C-S-H gel with partial substitution for calcium in its structure and interlayer; and physical encapsulation within the dense hydrate matrix, which limits the access of the extraction fluid to the metal-bearing phases (Chen et al. 2009; Ouhadi et al. 2021). Arsenic is fixed by a different route because it occurs as an oxyanion: it precipitates as calcium arsenate compounds, which the large calcium hydroxide reserve of the matrix makes possible, and is taken up by anion exchange in ettringite and the AFm phases, where arsenate substitutes for sulfate. Both routes are efficient at the concentrations involved here, and the small rise in the lead released at the highest sludge dosages (Fig. 5) simply reflects the greater metal load and the more porous matrix obtained at those levels.

Chromium fails for a specific chemical reason. In electroplating sludge, it derives largely from chromic acid and chromate plating baths and is therefore present to a significant extent as Cr(VI), which exists as the chromate and hydrogen chromate oxyanions (Chen et al. 2020). These species do not precipitate as hydroxides, so the alkalinity that immobilizes Cd, Pb, Ni and Cu offers them no advantage, and chromate remains soluble in alkaline media. The only sinks available in an OPC/RHA system are substitution for sulfate in ettringite and the AFm phases and a limited, reversible uptake by the C-S-H gel, and the sulfate already supplied by the cement and by the sludge (SO_3 = 2.35 % in both, Table 2) competes for the same sites. Under the TCLP protocol the acetic acid extraction fluid drives the eluate to pH 5.7-6.2 (Table 7), a range in which ettringite and the AFm phases are no longer stable and the C-S-H is progressively decalcified, so that chromate previously bound is released; the sensitivity of cement-solidified electroplating sludge to acid attack, and the associated loss of acid neutralization capacity, have been documented directly by Chen et al. (2009). No reducing agent is present to convert Cr(VI) into Cr(III), which would precipitate as the highly insoluble $Cr(OH)_3$. These factors together explain why chromium exceeds the limit in every sludge-bearing mix and why the exceedance widens as the sludge dosage increases in both panels of Fig. 5.

Nickel and copper are cationic and are retained by the same mechanisms as cadmium and lead, yet they are released at much higher concentrations. The difference is one of loading rather than of mechanism: the raw sludge contains more than 3 wt % nickel and leached 4125 mg/L of copper (Table 5), so the retention capacity of the matrix is saturated, and nickel hydroxide is appreciably more soluble than lead hydroxide in the mildly acidic range imposed by the extraction fluid. Fig. 5 also shows that, at a given sludge dosage, the mixes containing 10 % RHA release less chromium and less nickel than their 5 % RHA counterparts, for example 5.6 against 9.0 mg/L of chromium at ES/CEM = 25 % and 11.0 against 13.1 mg/L at 75 %. This is consistent with the pozzolanic formation of additional C-S-H of lower calcium-to-silicon ratio and with a refined pore structure, both of which increase the number of sorption sites and reduce the accessibility of the matrix (Asavapisit and Macphee 2007; Chiu et al. 2019); the effect is

systematic but far too small to bring chromium below the regulatory threshold. The benefit does not extend to every element, however: at the highest dosage, mix B4 released more lead and more cadmium than A4 (3.0 against 1.0 and 0.1 against < 0.005 mg/L), which is consistent with the much weaker and more porous matrix obtained in Group B at that loading, where the 28-day strength was only 0.45 MPa.

Overall, the matrix immobilized Cd, Pb, and As effectively but did not bring Cr within regulatory limits. Because the cause is the oxidation state of the chromium rather than the quality of the binder, the most direct route to compliance is the reduction of Cr(VI) to Cr(III) before or during solidification, for example by adding ferrous sulfate, a sulfide-bearing ground granulated blast furnace slag or zero-valent iron, after which chromium can be retained as an insoluble trivalent hydroxide; alkali-activated slag binders have been shown to perform well for chromium-bearing electroplating sludge for related reasons (Chen et al. 2020). This is an outcome that should be addressed before field application.

3.6 Limitations

First, the mechanistic interpretation offered in Sections 3.2 to 3.5 rests on the particle-size distribution of Fig. 1, on the oxide and loss-on-ignition data of Table 2, and on the strength and leaching behavior itself. Scanning electron microscopy and X-ray diffraction were outside the scope of the present work, so the microstructural changes and the hydrate assemblages invoked here — the metal hydroxide and metal silicate layers on the clinker grains, the substitution of chromate for sulfate in ettringite and the AFm phases, and the refinement of the pore structure by the pozzolanic reaction — were not observed directly. Confirming them would require a combined SEM/EDS and XRD program, ideally supplemented by thermogravimetric analysis of the calcium hydroxide reserve.

Second, the rice husk ash was characterized chemically but neither mineralogically nor physically. The combustion window of 550–600 °C was selected to preserve amorphous silica, and the behavior inferred from the strength and leaching results is consistent with that intention, but no X-ray diffraction pattern was recorded to confirm the absence of cristobalite and tridymite, and neither the Blaine fineness nor the specific surface area of the ash was measured. The pozzolanic contribution of the RHA is therefore established here only indirectly, through its effect on the mortars, and comparison with ashes produced elsewhere should be made with that in mind.

Third, the leaching assessment rests on a single batch extraction at one curing age. The TCLP is a short-term, worst-case screening test conducted under acetic acid conditions on crushed material, and it does not describe the release that would occur from a monolithic product over the service life of a structure. Dynamic or semi-dynamic tank leaching, sequential extraction to identify the binding fractions, and testing at later curing ages and after carbonation would be needed before a durable, field-scale conclusion on long-term containment could be drawn. Extending the program in these directions, and coupling it with the Cr(VI) reduction strategies identified in Section 3.5, is the natural continuation of this work.

4. Conclusion

This study examined the stabilization/solidification of electroplating sludge in cement-based mortars and the role of rice husk ash, evaluating fresh-state behavior, compressive strength, and heavy-metal leaching across twelve mixes. The raw electroplating sludge is unambiguously hazardous. Under the same TCLP protocol later applied to the mortars, its leachate exceeded at least one regulatory threshold for every metal determined, which justifies a stabilization/solidification approach. The effect of the sludge on the fresh mortar depended on its role. Used as a fine-aggregate replacement, it raised the slump from 75 mm for the control mortar to 150 mm at 35 % replacement, improving workability, whereas when added to the binder, it retarded both the initial and the final setting times, an effect amplified by a higher RHA content (10 % against 5 %); the delays nonetheless remained within practical limits, at most 420 min for the initial and 510 min for the final set. Compressive strength fell sharply once sludge entered the binder, from 16.3-29.0 MPa for the sludge-free mixes to 0.30-6.1 MPa at ES/CEM ratios of 25-75 %, and the 28- and 90-day values were almost identical in the sludge-bearing mixes, so that no late-age recovery should be expected. Used as a fine-aggregate replacement, ES preserved markedly higher strength, from 15.5 MPa at 15 % to 6.4 MPa at 35 %, against 29.0 MPa for the plain reference mortar. TCLP testing showed that cadmium, lead and arsenic were immobilized below their US EPA regulatory levels, whereas chromium exceeded the 5 mg/L limit in all sludge-bearing mixes because it is present as the chromate oxyanion, which the alkalinity of a cement matrix cannot precipitate; reduction of Cr(VI) to Cr(III) is therefore the priority for further work.

Statements and Declarations

Acknowledgements
The authors thank the staff of the Pirouz Shomal industrial wastewater treatment plant for providing the electroplating sludge used in this study.

Ethical considerations
Ethical issues (Including plagiarism, informed consent, misconduct, data fabrication and/or falsification, double publication and/or submission, redundancy, etc.) have been completely observed by the author.

Data availability
Data will be made available on request.

Conflicts of interest
The author declares that they have no known competing financial interests or personal relationships that could have appeared to influence the work reported in this paper.

Author contribution
S. Shams: Writing the main Draft; S. Gitipour: Conceptualization; Writing – Review & Editing; and A. M. Baghdadi: Conceptualization, Methodology, Review, and Final Proof.

AI Use Declaration
During the preparation of this manuscript, the authors used AI tools for designing the Graphical Abstract. All content has

been carefully reviewed and revised by the authors, who take full responsibility for the final version of the manuscript.

References

Adenuga, A. A., Amos, O. D., Oyekunle, J. A. O., & Umukoro, E. H. (2019). Adsorption performance and mechanism of a low-cost biosorbent from spent seedcake of *Calophyllum inophyllum* in simultaneous cleanup of potentially toxic metals from industrial wastewater. *Journal of Environmental Chemical Engineering, 7*(5), 103317. https://doi.org/10.1016/j.jece.2019.103317

Asavapisit, S., & Macphee, D. E. (2007). Immobilization of metal-containing waste in alkali-activated lime–RHA cementitious matrices. *Cement and Concrete Research, 37*(5), 776–780. https://doi.org/10.1016/j.cemconres.2007.02.003

ASTM International. (2003). *Standard test method for slump of hydraulic cement concrete* (ASTM C143/C143M-03). https://doi.org/10.1520/C0143_C0143M-03ASTM International. (2005). Standard specification for coal fly ash and raw or calcined natural pozzolan for use in concrete (ASTM C618-05).

ASTM International. (2008). *Standard test methods for time of setting of hydraulic cement by Vicat needle* (ASTM C191-08). https://doi.org/10.1520/C0191-08

ASTM International. (2009). *Standard test method for density (unit weight), yield, and air content (gravimetric) of concrete* (ASTM C138/C138M-09). https://doi.org/10.1520/C0138_C0138M-09

ASTM International. (2011). *Standard practice for mechanical mixing of hydraulic cement pastes and mortars of plastic consistency* (ASTM C305-11). https://doi.org/10.1520/C0305-11

ASTM International. (2016). *Standard test method for compressive strength of hydraulic cement mortars (using 2-in. or [50-mm] cube specimens)* (ASTM C109/C109M-16a). https://doi.org/10.1520/C0109_C0109M-16A

Balali-Mood, M., Naseri, K., Tahergorabi, Z., Khazdair, M. R., & Sadeghi, M. (2021). Toxic mechanisms of five heavy metals: Mercury, lead, chromium, cadmium, and arsenic. *Frontiers in Pharmacology, 12*, 643972. https://doi.org/10.3389/fphar.2021.643972

Bocanegra, J. J. C., Mora, E. E., & González, G. I. C. (2019). Galvanic sludges: Effectiveness of red clay ceramics in the retention of heavy metals and effects on their technical properties. *Environmental Technology & Innovation, 16*, 100459. https://doi.org/10.1016/j.eti.2019.100459

Chandrasekhar, S., Satyanarayana, K. G., Pramada, P. N., Raghavan, P., & Gupta, T. N. (2003). Review: Processing, properties and applications of reactive silica from rice husk—an overview. *Journal of Materials Science, 38*(15), 3159–3168. https://doi.org/10.1023/A:1025157114800

Chang, J. E., Lin, T. T., Ko, M. S., & Liaw, D. S. (1999). Stabilization/solidification of sludges containing heavy metals by using cement and waste pozzolans. *Journal of Environmental Science and Health, Part A: Toxic/Hazardous Substances and Environmental Engineering, 34*(5), 1143–1160. https://doi.org/10.1080/10934529909376887

Chen, H., Yuan, H., Mao, L., Hashmi, M. Z., Xu, F., & Tang, X. (2020). Stabilization/solidification of chromium-bearing electroplating sludge with alkali-activated slag binders. *Chemosphere, 240*, 124885. https://doi.org/10.1016/j.chemosphere.2019.124885

Chen, Q., Zhang, L., Ke, Y., Hills, C., & Kang, Y. (2009). Influence of carbonation on the acid neutralization capacity of cements and cement-solidified/stabilized electroplating sludge. *Chemosphere, 74*(6), 758–764. https://doi.org/10.1016/j.chemosphere.2008.10.044

Chen, R., Cai, G., Dong, X., Pu, S., Dai, X., & Duan, W. (2022). Green utilization of modified biomass by-product rice husk ash: A novel eco-friendly binder for stabilizing waste clay as road material. *Journal of Cleaner Production, 376*, 134303. https://doi.org/10.1016/j.jclepro.2022.134303

Chen, Y. L., Chang, J. E., Lai, Y. C., & Ko, M. S. (2012). Effects of sintering atmosphere on cement clinkers produced from chromium-bearing sludge. *Journal of the Air & Waste Management Association, 62*(5), 587–593. https://doi.org/10.1080/10962247.2012.665012

Chiu, A. C., Akesseh, R., Moumouni, I. M., & Xiao, Y. (2019). Laboratory assessment of rice husk ash (RHA) in the solidification/stabilization of heavy metal contaminated slurry. *Journal of Hazardous Materials, 371*, 62–71. https://doi.org/10.1016/j.jhazmat.2019.02.051

Dai, Z., Wu, Y., Hu, L., Zhang, W., & Mao, L. (2019). Evaluating physical-mechanical properties and long periods environmental risk of fired clay bricks incorporated with electroplating sludge. *Construction and Building Materials, 227*, 116716. https://doi.org/10.1016/j.conbuildmat.2019.116716

Della, V. P., Kühn, I., & Hotza, D. (2002). Rice husk ash as an alternate source for active silica production. *Materials Letters, 57*(4), 818–821. https://doi.org/10.1016/S0167-577X(02)00879-0

Deng, Y., & Zhao, R. (2015). Advanced oxidation processes (AOPs) in wastewater treatment. *Current Pollution Reports, 1*(3), 167–176. https://doi.org/10.1007/s40726-015-0015-z

Deutsches Institut für Normung. (2016). *Methods of testing cement—Part 1: Determination of strength* (DIN EN 196-1:2016-11). https://doi.org/10.31030/2482416

Fathollahi, R., Shahmoradi, M., Babamoradi, R., & Abkhiz, M. (2025, December 17–19). *Investigation of the effect of rice husk ash as a pozzolan on the compressive strength of high strength concrete produced with local materials of Ilam* [Paper presentation]. 11th National Congress on Civil Engineering, Architecture, Art and Urban Development, Tehran, Iran (In Persian). https://civilica.com/doc/2666534

Hashim, A. A., Abdul Kadir, A., Sarani, N. A., Hassan, M. I. H., Kersnansamy, A., & Abdullah, M. M. A. B. (2022). Immobilization of metals in fired clay brick incorporated with aluminium-rich electroplating sludge: Properties and

leaching analysis. *Sustainability, 14*(14), 8732. https://doi.org/10.3390/su14148732

Jafarpour, F., Majedi, M. H., & Ramezanianpour, A. (1997). Making of masonry cement with rice husk. Building and Housing Research Center, Tehran, Iran. (In Persian).

Jochem, L. F., Casagrande, C. A., Bizinotto, M. B., Aponte, D., & Rocha, J. C. (2021). Study of the solidification/stabilization process in a mortar with lightweight aggregate or recycled aggregate. *Journal of Cleaner Production, 326*, 129415. https://doi.org/10.1016/j.jclepro.2021.129415

Kamar, M. T., Elattar, H., Mahmoud, A. S., Peters, R. W., & Mostafa, M. K. (2024). A critical review of state-of-the-art technologies for electroplating wastewater treatment. *International Journal of Environmental Analytical Chemistry, 104*(16), 4143–4176. https://doi.org/10.1080/03067319.2022.2098486

Li, H., Yang, X., Suo, Z., Xia, Y., & He, D. (2014). Red cement-based decorative mortar prepared with dry electroplating sludge containing Pb as red pigment. *Journal of Wuhan University of Technology-Materials Science Edition, 29*(2), 291–297. https://doi.org/10.1007/s11595-014-0910-y

Liew, A. G., Idris, A., Samad, A. A., Wong, C. H. K., Jaafar, M. S., & Baki, A. M. (2004). Reusability of sewage sludge in clay bricks. *Journal of Material Cycles and Waste Management, 6*(1), 41–47. https://doi.org/10.1007/s10163-003-0105-7

Miao, J., Wang, J., Sun, C., Liu, X., Fu, H., & Xia, Y. (2025). Stabilization/solidification of nickel-containing electroplating sludge by sustainable geopolymer: Mechanism and applicability. *Journal of Environmental Chemical Engineering, 13*(3), 115717. https://doi.org/10.1016/j.jece.2025.115717

Momeni, K., & Ghorbani Kamsari, H. (2025, August 13). *Investigation of the effect of rice husk ash (RHA) on the mechanical properties and durability of high performance concrete (HPC)* [Paper presentation]. 4th International Conference on Architecture, Civil Engineering, Urbanism, Environment and Horizons of Islamic Art, Tabriz, Iran. https://civilica.com/doc/2429050

Momotko, M., Koundle, P., Latif, S., Ilyas, M., Samejo, B. A., Imran, M., Yin, Z., Zhan, J., Kong, L., Boczkaj, G., & Nirmalkar, N. (2025). Advanced oxidation processes (AOPs) in wastewater treatments. In R. Castro-Muñoz, A. Basile, A. Cassano, & S. De (Eds.), *Advanced technologies in wastewater treatment: Food, pharmaceutical and chemical industry* (pp. 79–114). Elsevier. https://doi.org/10.1016/B978-0-443-26500-6.00004-3

Monosi, S., Ruello, M. L., & Sani, D. (2016). Electric arc furnace slag as natural aggregate replacement in concrete production. *Cement and Concrete Composites, 66*, 66–72. https://doi.org/10.1016/j.cemconcomp.2015.10.004

Monzó, J., Payá, J., Borrachero, M. V., & Córcoles, A. (1996). Use of sewage sludge ash (SSA)-cement admixtures in mortars. *Cement and Concrete Research, 26*(9), 1389–1398. https://doi.org/10.1016/0008-8846(96)00119-6

Ouhadi, V. R., Yong, R. N., & Deiranlou, M. (2021). Enhancement of cement-based solidification/stabilization of a lead-contaminated smectite clay. *Journal of Hazardous Materials, 403*, 123969. https://doi.org/10.1016/j.jhazmat.2020.123969

Petrillo, A., Fraternali, F., Acampora, A., Di Chiara, G., Colangelo, F., & Farina, I. (2025). Innovative solidification and stabilization techniques using industrial by-products for soil remediation. *Applied Sciences, 15*(7), 4002. https://doi.org/10.3390/app15074002

Rajoria, S., Vashishtha, M., & Sangal, V. K. (2021). Review on the treatment of electroplating industry wastewater by electrochemical methods. *Materials Today: Proceedings, 47*, 1472–1479. https://doi.org/10.1016/j.matpr.2021.04.165

Rajoria, S., Vashishtha, M., & Sangal, V. K. (2025). Electroplating industry wastewater treatment: Advanced electrochemical oxidation process. In S. Souabi, A. Anouzla, S. Yadav, V. P. Singh, & R. N. Yadava (Eds.), *Wastewater treatment plants: Processes, assessment, design and operation* (pp. 421–438). Springer. https://doi.org/10.1007/978-3-031-87461-1_16

Tavares, C. R. G., & de Melo Franco, J. (2012). Production of concrete paving blocks (CPB) utilising electroplating residues: Evaluation of mechanical and micro-structural properties. *The Canadian Journal of Chemical Engineering, 90*(5), 1092–1101. https://doi.org/10.1002/cjce.21677

U.S. Environmental Protection Agency. (1992). *Method 1311: Toxicity characteristic leaching procedure* (Test Methods for Evaluating Solid Waste, Physical/Chemical Methods, SW-846, 3rd ed.). Office of Solid Waste. https://www.epa.gov/sites/default/files/2015-12/documents/1311.pdf

Velumani, P., & Senthilkumar, S. (2018). Production of sludge-incorporated paver blocks for efficient waste management. *Journal of the Air & Waste Management Association, 68*(6), 626–636. https://doi.org/10.1080/10962247.2017.1395373

Wang, D. X., Abriak, N. E., Zentar, R., & Xu, W. (2012). Solidification/stabilization of dredged marine sediments for road construction. *Environmental Technology, 33*(1), 95–101. https://doi.org/10.1080/09593330.2011.551840

Wang, H., Liu, X., & Zhang, Z. (2024). Approaches for electroplating sludge treatment and disposal technology: Reduction, pretreatment and reuse. *Journal of Environmental Management, 349*, 119535. https://doi.org/10.1016/j.jenvman.2023.119535

Wang, J., Miao, J., Shi, D., Zhang, J., Zhao, Y., & Xia, Y. (2025). Sustainable stabilization/solidification of electroplating sludge using a low-carbon ternary cementitious binder. *Journal of Environmental Chemical Engineering, 13*(2), 115022. https://doi.org/10.1016/j.jece.2025.115022

Yaghoubi, H., Allahyari, M. S., Firouzi, S., Damalas, C. A., & Marzban, S. (2019). Identifying sustainable options for rice husk valorization using the analytic hierarchy process.

Outlook on Agriculture, 48(2), 117–125. https://doi.org/10.1177/0030727018821384

Yu, C., Zhang, Y., Liu, Y., Zhu, S., Liang, D., Sun, T., Xie, X., & Wang, X. (2022). Resource utilization of hazardous Cr/Fe-rich sludge: Synthesis of erdite flocculant to treat real electroplating wastewater. *Journal of Environmental Health Science and Engineering, 20*(1), 509–519. https://doi.org/10.1007/s40201-022-00796-0

Zhang, Y., Shi, P., Chen, L., & Tang, Q. (2018). Utilization of electroplating sludge as subgrade backfill materials: Mechanical and environmental risk evaluation. *Advances in Civil Engineering, 2018*, 4891418. https://doi.org/10.1155/2018/4891418

Ziyari, M., & Mostakhdemin Hosseini, M. R. (2025, January 6–8). *Investigation of the effects of pozzolanic materials on the behavior of high performance self compacting concrete* [Paper presentation]. 11th National Congress on Civil Engineering, Architecture, Art and Urban Development, Tehran, Iran (In Persian). https://civilica.com/doc/2667079

© Authors, Published by *Environmental Health and Pollution Research*. This is an open-access article distributed under the CC BY (license: http//creativecommons.org.licenses.by.4.0).